Numerical Approach to Stochastic Neural Fields

Pedro M. Lima

CENTER FOR COMPUTATIONAL MATHEMATICS AND STOCHASTICS
INSTITUTO SUPERIOR TÉCNICO
UNIVERSITY OF LISBON
PORTUGAL

November 30, 2022

OUTLINE OF LECTURE

- Introduction: sources of noise in neural activity
- Stochastic neural field equation
- Numerical methods
- Numerical results
- Conclusion

MOTIVATION FOR STOCHASTIC MODELS

Sources of noise in neural fields:

- Irregularity of spikes
- Non-homogeneous or irregular connectivity
- Perturbations of external stimulus

Questions we would like to answer by means of stochastic models:

- Does noise interfere in the existence of stationary solutions?
- How far the stationary solutions can be modified as a result of noise?
- May a stationary solution be transformed into another one just as a result of noise? What is the probability that this happens?

See for example Kilpatrick and Ermentrout (2012); Thul, Coombes Laing (2016)

STOCHASTIC MODELS

NFE with Additive Noise:

$$dU_t(x) = \left(I(x,t) - \alpha U_t(x) + \int_\Omega K(|x-y|) S(U_t(y)) dy \right) dt + \epsilon dW_t(x), \tag{1}$$

where $t \in [0, T]$, $x \in \Omega \subset \mathbb{R}^n$, W_t is a Q-Wiener process.

Kuhn and Riedler, 2014

We will consider domains of the form $\Omega = [-l, l]$, including the limit case when $l \to \infty$.

NUMERICAL APPROXIMATION

To construct a numerical approximation of the solution of SNFE in the one-dimensional case, we begin by expanding the solution $U_t(x)$ using the Karhunen-Loeve formula:

$$U_t(x) = \sum_{k=0}^{\infty} u_t^k v_k(x), \tag{2}$$

v_k eigenfunctions of the covariance operator of the noise- orthogonal system;

How to compute the coefficients u_t^k ?

$$\begin{aligned}(dU_t, v_i) = \big[(I(x,t), v_i) - \alpha(U_t, v_i) + \\ + \left(\int_\Omega K(|x-y|)S(U_t(y))dy, v_i\right)\big]\, dt + \epsilon(dW_t, v_i).\end{aligned} \tag{3}$$

We expand dW_t as

$$dW_t(x) = \sum_{k=0}^{\infty} v_k(x)\lambda_k d\beta_t^k, \tag{4}$$

β_t^k - system of independent white noises in time ;

λ_k - eigenvalues of the covariance operator of the noise.

NUMERICAL APPROXIMATION

We consider:

$$EW_t(x)W_s(y) = \min(t,s)\frac{1}{2\xi}\exp\left(\frac{-\pi}{4}\frac{|x-y|^2}{\xi^2}\right),$$

where ξ - spatial correlation length. If $\xi << 2l$, the eigenvalues of the covariance operator satisfy

$$\lambda_k^2 = \exp\left(-\frac{\xi^2 k^2}{4\pi}\right).$$

Based on the ortogonality of the system v_k, we obtain

$$du_t^i = \left[(I(x,t),v_i) - \alpha u_t^i + (KS)^i(\bar{u}_t)\right]dt + \epsilon\lambda_i d\beta_t^i, \tag{5}$$

where $(KS)^i(\bar{u}_t)$ denotes the nonlinear term of the system:

$$(KS)^i(\bar{u}_t) = \int_\Omega v_i(x)\left(\int_\Omega K(|x-y|)S\left(\sum_{k=1}^{\infty} u_t^k v_k(y)\right)dy\right)dx. \tag{6}$$

NUMERICAL APPROXIMATION- GALERKIN METHOD

When using the Galerkin method we define an approximate solution :

$$U_t^N(x) = \sum_{k=0}^{N-1} u_t^{k,N} v_k(x). \tag{7}$$

Then the coefficients $u_t^{k,N}$ satisfy the following nonlinear system of stochastic delay differential equations:

$$du_t^{i,N} = \left[(I(x,t), v_i) - \alpha u_t^{i,N} + (KS)^{i,N}(\bar{u}_t) \right] dt + \epsilon \lambda_i d\beta_t^i, \tag{8}$$

where $(KS)^{i,N}(\bar{u}_t)$ is given by

$$(KS)^{i,N}(\bar{u}_t) = h^2 \sum_{l=1}^{N} v_i(x_l) \left(\sum_{j=1}^{N} K(|x_l - x_j|) S \left(\sum_{k=1}^{N} u_t^k v_k(x_j) \right) \right) \tag{9}$$

$i = 0, \ldots, N-1$. In this case we are introducing in $[-L, L]$ a set of $N+1$ equidistant gridpoints $x_j = -l + j * h$, $j = 0, \ldots, N$, where $h = 2L/N$, and using the rectangular rule to evaluate the integral in (6).

NUMERICAL APPROXIMATION - EULER-MARUYAMA METHOD

Uniform mesh with step size h_t: $t_j = jh_t$, $j = 0, 1, ..., n$.

Approximate solution:

$$(u_1^{k,N}, u_2^{k,N}, ..., u_n^{k,N}),$$

where

$$u_j^{k,N} \approx u_{t_j}^{k,N}.$$

Euler-Maruyama method

$$u_{j+1}^{i,N} = u_j^{i,N} + h_t \left[(I(x_i, t_j), v_i) - \alpha u_{j+1}^{i,N} + (KS)^{i,N}(\bar{u}_{t_j}) \right] + \sqrt{h_t} \epsilon \lambda_i w_i, \tag{10}$$

where w_i is a random variable with normal distribution $(w_i = N(0, 1))$, $j = 0, ..., n$, $i = 0, ..., N-1$.

Semi-implicit version of the Euler-Maruyama method:

$$u_{j+1}^{i,N} = \frac{u_j^{i,N} + h_t \left[(I(x_i, t_j), v_i) + (KS)^{i,N}(\bar{u}_{t_j}) \right] + \sqrt{h_t} \epsilon \lambda_i w_i}{1 + \alpha h_t}. \tag{11}$$

NUMERICAL APPROXIMATION - CHOICE OF THE BASIS FUNCTIONS

$$v_k(x) = \exp(ikx), \qquad k = 0, 1, .., N. \tag{12}$$

Note that with this choice of the basis functions the inner products and the sums in the computations can be interpreted as the Discrete Fourier Transform (DFT).

$(I(x, t_j), v_i)$, $i = 1, ..., N$ -DFT of the vector I_N, which contains the values of the function $I(x, t)$ at the grid points $x_k = -l + kh$, $k = 1, .., N$.

The inner products can be evaluated efficiently by the Fast Fourier Transform (FFT).

NUMERICAL RESULTS - DETERMINISTIC CASE

Input data: Connectivity:

$$K(x) = 2\exp(-0.08x)\left(0.08\sin(\pi x/10) + \cos(\pi x/10)\right).$$

External input:

$$I(x) = -3.39967 + 8\exp\left(-\frac{x^2}{18}\right).$$

Firing rate - Heaviside function.

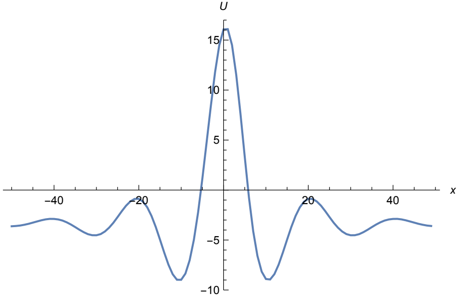

Example 1:stationary one-bump solution.

NUMERICAL RESULTS - DETERMINISTIC CASE

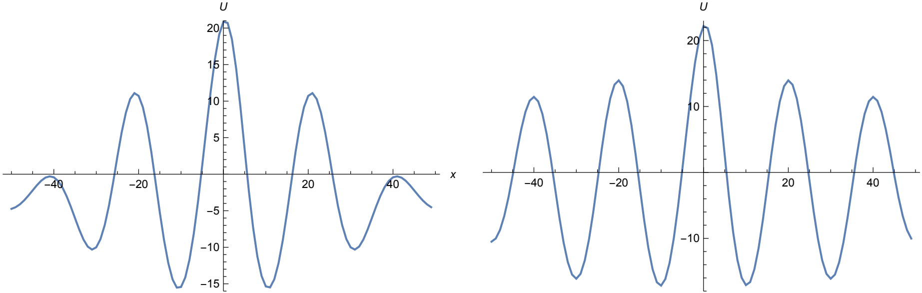

Example 1: Stationary three-bump (left) and five-bump (right) solutions. The deterministic case supports different kinds of stationary solutions, which can be obtained by changing the initial conditions.
Technical details: $h_t = 0.02$, $n = 200$, $I = [-50, 50]$, $N = 100$, $h = 1$.

NUMERICAL RESULTS - STOCHASTIC CASE

Notations:

$$U_{max,max}(t) = \max_{s\in\{1,\dots,n_p\}} \max_{i\in\{1,\dots,N\}} u(s, x_i, t);$$

$$U_{min,max}(t) = \min_{s\in\{1,\dots,n_p\}} \max_{i\in\{1,\dots,N\}} u(s, x_i, t);$$

$$U_{max,min}(t) = \max_{s\in\{1,\dots,n_p\}} \min_{i\in\{1,\dots,N\}} u(s, x_i, t);$$

$$U_{min,min}(t) = \min_{s\in\{1,\dots,n_p\}} \min_{i\in\{1,\dots,N\}} u(s, x_i, t);$$

We consider the following approximations of mathematical expectations:

$$E(u(x,t)) \approx \frac{1}{n_p} \sum_{s=1}^{n_p} u(s, x, t);$$

$$E(\max_{x\in[-l,l]} u(x,t)) \approx E_{max}(t) = \frac{1}{n_p} \sum_{s=1}^{n_p} \max_{i\in\{1,\dots,N\}} u(s, x_i, t);$$

$$E(\min_{x\in[-l,l]} u(x,t)) \approx E_{min}(t) = \frac{1}{n_p} \sum_{s=1}^{n_p} \min_{i\in\{1,\dots,N\}} u(s, x_i, t);$$

NUMERICAL RESULTS - STOCHASTIC CASE

Example 2 : $\epsilon = 0.01$, $U_0 \equiv 0$.

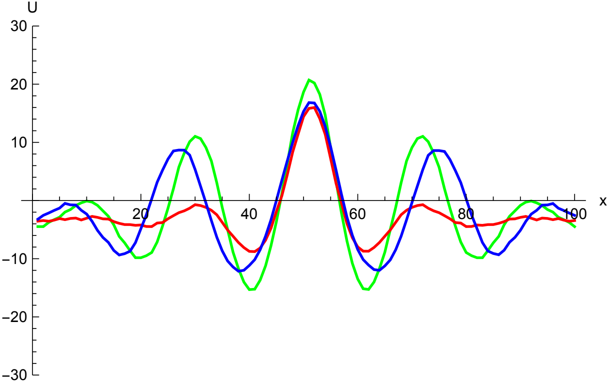

Three paths of the solution with $\epsilon = 0.01$, at $t = 4$. Technical details: $h_t = 0.02$, $n = 200$, $I = [-50, 50]$, $N = 100$, $h = 1$, $n_p = 100$.

NUMERICAL RESULTS - STOCHASTIC CASE

Example 2 : $\epsilon = 0.01$, $U_0 \equiv 0$.

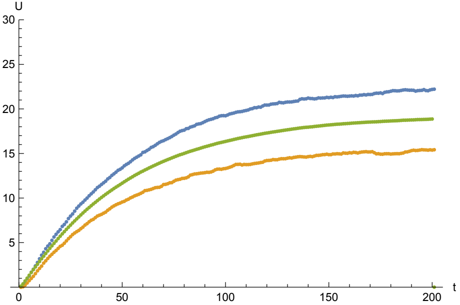

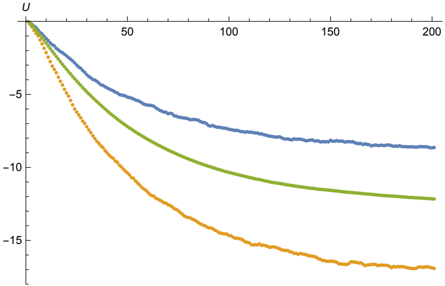

Left: Evolution of $U_{max,max}$ (blue), $U_{min,max}$ (yellow)E_{max} (green).
Right: Evolution of $U_{max,min}$ (blue), $U_{min,min}$ (yellow), E_{min} (green).
Technical details:
$h_t = 0.02$, $n = 200$, $I = [-50, 50]$, $N = 100$, $h = 1$, $n_p = 100$.

NUMERICAL RESULTS - STOCHASTIC CASE

Example 2 : $\epsilon = 0.01$, $U_0 \equiv 0$.

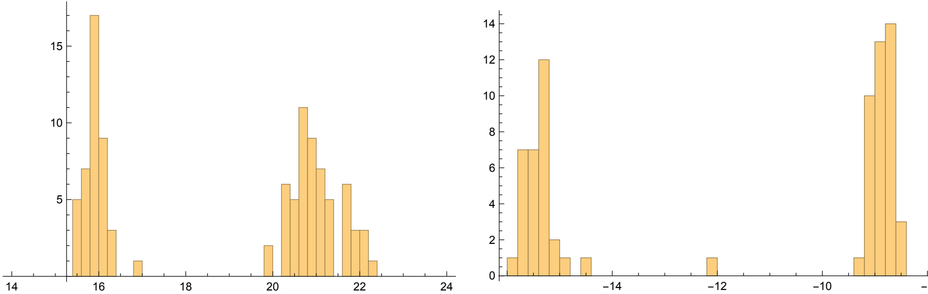

Histograms of distribution of u_{max} (left) and u_{min} (right), as $t = 4$.

NUMERICAL RESULTS - STOCHASTIC CASE

Example 3 : $\epsilon = 0.05$, $U_0 \equiv 0$.

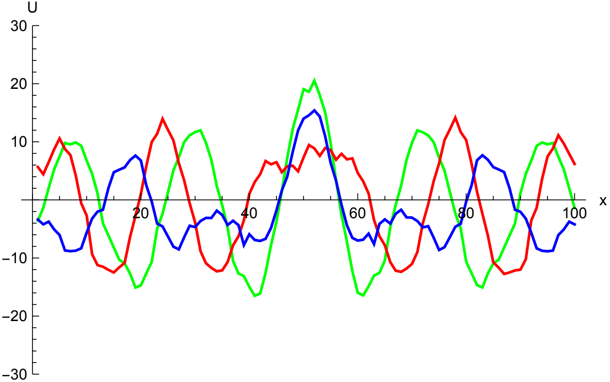

Three paths of the solution with $\epsilon = 0.05$, at $t = 4$. Technical details: $h_t = 0.02$, $n = 200$, $I = [-50, 50]$, $N = 100$, $h = 1$, $n_p = 100$.

NUMERICAL RESULTS - STOCHASTIC CASE

Example 3: $\epsilon = 0.05$, $U_0 \equiv 0$.

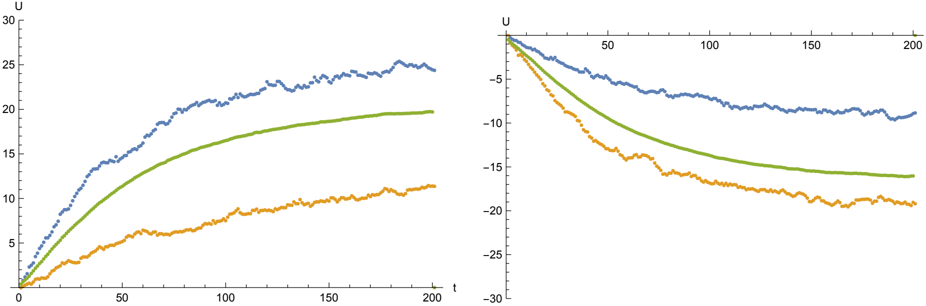

Left: Evolution of $U_{max,max}$ (blue), $U_{min,max}$ (yellow) , E_{max} (green).
Right: Evolution of $U_{max,min}$, $U_{min,min}$, E_{min}.

NUMERICAL RESULTS - STOCHASTIC CASE

Example 3 : $\epsilon = 0.05$, $U_0 \equiv 0$.

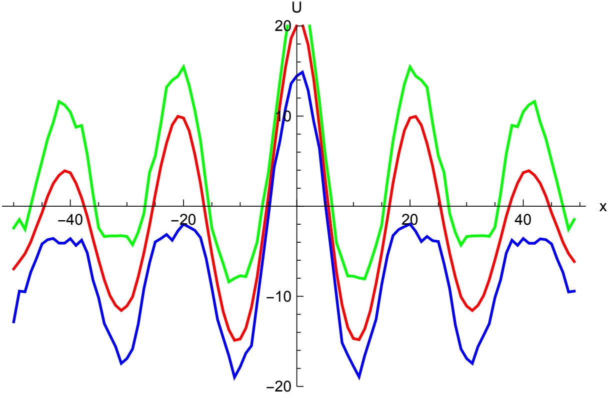

Graph of $E(u(x,4))$ (red line), $\max_{s \in \{1,\dots,100\}} u(s,x,4)$ (green line) and $\min_{s \in \{1,\dots,100\}} u(s,x,4)$ (blue line). at $t = 4$.

NUMERICAL RESULTS - STOCHASTIC CASE

Example 3 : $\epsilon = 0.05$, $U_0 \equiv 0$.

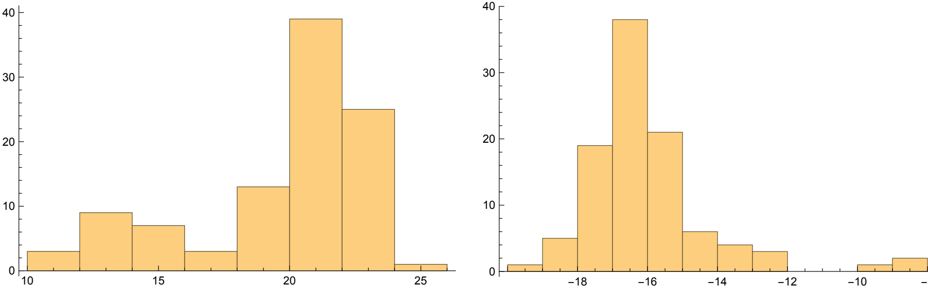

Histograms of distribution of u_{max} (left) and u_{min} (right), as $t = 4$.

NUMERICAL RESULTS - STOCHASTIC CASE

Example 4 : $\epsilon = 0.01$, U_0 – one-bump solution.

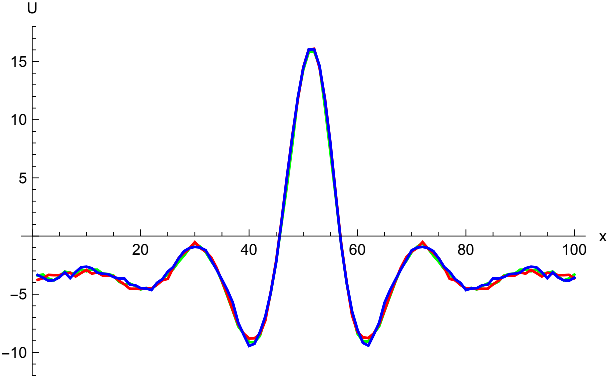

Three paths of the solution at $t = 4$. Technical details:
$h_t = 0.02, n = 200, I = [-50, 50], N = 100, h = 1, n_p = 100.$

NUMERICAL RESULTS - STOCHASTIC CASE

Example 4 : $\epsilon = 0.01$, U_0 – one-bump solution.

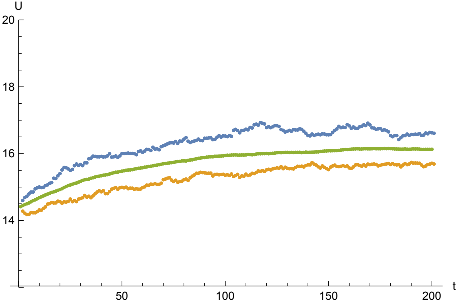

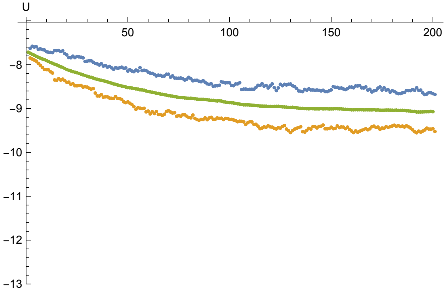

Left: Evolution of $U_{max,max}$ (blue), $U_{min,max}$ (yellow) , E_{max} (green).
Right: Evolution of $U_{max,min}$, $U_{min,min}$, E_{min}.

NUMERICAL RESULTS - STOCHASTIC CASE

Example 4: $\epsilon = 0.01$, U_0 - one-bump solution.

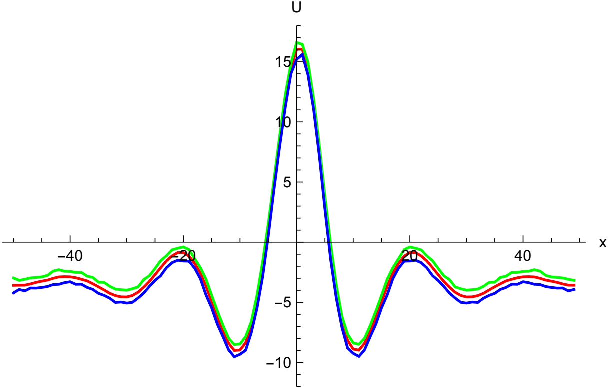

Graph of $E(u(x,4))$ (red line), $\max_{s\in\{1,\dots,100\}} u(s,x,4)$ (green line) and $\min_{s\in\{1,\dots,100\}} u(s,x,4)$ (blue line).

NUMERICAL RESULTS - STOCHASTIC CASE

Example 4 : $\epsilon = 0.01$, U_0 – one-bump solution.

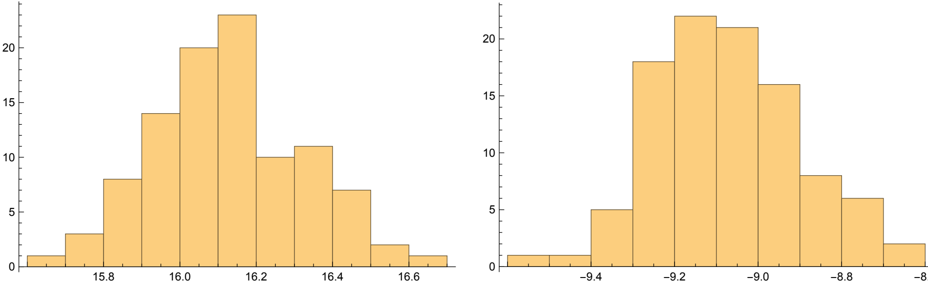

Histograms of distribution of u_{max} (left) and u_{min} (right), as $t = 4$.

NUMERICAL RESULTS - STOCHASTIC CASE

Number of zeroes of stochastic trajectories

zeroes	$\epsilon = 0.01$	$\epsilon = 0.01$	$\epsilon = 0.05$	$\epsilon = 0.05$
	$U_0 \equiv 0$	U_0- one bump	$U_0 \equiv 0$	U_0 -one bump
2	**41**	**100**	0	0
3	0	0	0	0
4	0	0	0	0
5	0	0	0	0
6	24	0	4	20
7	0	0	0	1
8	34	0	12	0
9	0	0	7	0
10	0	0	**76**	**76**
11	0	0	0	0
12	0	0	1	0
14	0	0	0	3

(13)

CONCLUSIONS

- At a low level of noise the trajectories of the stochastic equation are concentrated near the stationary solutions of the deterministic one.
- In particular, if the initial condition is the null function, in the presence of not very strong noise ($\epsilon = 0.01$) the trajectories of the stochastic equation split into two classes, each of them close to a certain stationary solution of the deterministic equation. In other words, the stationary solutions of the deterministic case play the role of attractors for the trajectories of the stochastic case.
- If the initial condition is a one-bump stationary solution, in the case of not very strong noise most of the trajectories of the stochastic equation are of the same type as the stationary solution and only a few are transformed into solutions of different types.

CONCLUSIONS AND PROBLEMS UNDER INVESTIGATION

- In the case of strong noise ($\epsilon = 0.05$) the trajectories of the stochastic equation may take very different forms and it is difficult to compare them with the stationary solutions of the deterministic case.
- Moreover, in the case of strong noise it seems that the behaviour of the trajectories of the stochastic equation does not strongly depend on the the initial condition.
- The joint effect of noise and delay in the solutions of the NFE is a current field of research.
- Stochastic two-dimensional neural fields are also under investigation.

REFERENCES

- A. Hutt and N. Rougier, Activity spread and breathers induced by finite transmission speeds in two-dimensional neuronal fields, Physical Review,E 82 (2010) 055701.
- P.M. Lima and E. Buckwar, Numerical solution of the neural field equations in the two-dimensional case, SIAM J. Sci. Comput. , 37 , N.6 (2015) B962-B979.
- C. Kühn and M.G. Riedler, Large deviations for nonlocal stochastic neural fields, J. Math. Neurosci. 4:1 (2014) 1–33.
- Flora Ferreira, Multi-bump solutions in dynamic neural fields: analysis and applications, PhD thesis, University of Minho, 2014 (http://hdl.handle.net/1822/34416).
- Kilpatrick, Z. and Ermentrout, B.: Wandering bumps in stochastic neural fields, SIAM J. Appl. Dyn. Syst., **12** (2013) 61–94.